



Article

Application of Remote Sensing Techniques to Identification of Underwater Airplane Wreck in Shallow Water Environment: Case Study of the Baltic Sea, Poland

Artur Grządziel

Department of Navigation and Hydrography, Faculty of Navigation and Naval Weapons, Polish Naval Academy, 81-127 Gdynia, Poland; a.grzadziel@amw.gdynia.pl

Abstract: Multibeam echo sounders (MBES), side-scan sonars (SSS), and remotely operated vehicles (ROVs) are irreplaceable devices in contemporary hydrographic works. However, a highly reliable method of identifying detected wrecks is visual inspection through diving surveys. During underwater research, it is sometimes hard to obtain images in turbid water. Moreover, on-site diving operations are time-consuming and expensive. This article presents the results of the remote sensing surveys that were carried out at the site of a newly discovered wreck, in the southern part of the Baltic Sea (Poland). Remote sensing techniques can quickly provide a detailed overview of the wreckage area and thus considerably reduce the time required for ground truthing. The goal of this paper is to demonstrate the process of identification of a wreck based on acoustic data, without involving a team of divers. The findings, in conjunction with the collected archival documentation, allowed for the identification of the wreck of a Junkers Ju-88, a bomber from World War II.

Keywords: remote sensing; shallow water; seafloor mapping; underwater object; wreck identification



Citation: Grządziel, A. Application of Remote Sensing Techniques to Identification of Underwater Airplane Wreck in Shallow Water Environment: Case Study of the Baltic Sea, Poland. *Remote Sens.* **2022**, *14*, 5195. <https://doi.org/10.3390/rs14205195>

Academic Editors: Dimitrios Skarlatos, Gema Casal, Karantzas Konstantinos, Gottfried Mandlbürger and Panagiotis Agrafiotis

Received: 1 September 2022

Accepted: 15 October 2022

Published: 17 October 2022

Publisher's Note: MDPI stays neutral with regard to jurisdictional claims in published maps and institutional affiliations.



Copyright: © 2022 by the author. Licensee MDPI, Basel, Switzerland. This article is an open access article distributed under the terms and conditions of the Creative Commons Attribution (CC BY) license (<https://creativecommons.org/licenses/by/4.0/>).

1. Introduction

According to [1–3] it is estimated that there are about three million shipwrecks at the bottom of the world's seas and oceans. To date, only 19% of the world's oceans have been mapped, which means that much of the marine environment, including shipwreck sites, is still unexplored [4–6]. In the Baltic Sea area, the greatest number of recorded wrecks are found in Swedish waters. Out of 30,000 identified objects lying on the seabed, a significant part is classified as wrecks or wreck remains from different periods of navigation. Finland indicates the presence of 5200 wrecks in its waters, and in Denmark, the database of wrecks contains 2518 records, without distinguishing the level of risk to the environment. Polish records indicate the presence of over 400 wrecks [7]. The data held by the Hydrographic Office of the Polish Navy (HOPN) show that there are over 415 wrecks in the Polish sea areas, of which about 100 are located in the Bay of Gdańsk [8].

There are over 20,000 underwater objects on the sea bottom of the Baltic Sea in the Polish Exclusive Economic Zone (EEZ), with a still high number of new discoveries, including wrecks. The group of interested parties engaged in the exploration of wrecks includes divers, marine archaeologists, employees of the Maritime Institute, Maritime Offices, as well as the Maritime Museum.

The numerous Baltic shipwrecks scattered on the seabed originate from wars, violent storms, and miscalculation of skippers and captains. These objects are considered an essential part of our cultural heritage and are part of our collective planetary history. They play an important role from the scientific, political, cultural, and economic point of view [9,10]. The presence of a large number of well-preserved wrecks was influenced by geographical, historical and political factors. The geographic and hydrological conditions of the Baltic Sea, such as low salinity and low water temperatures, have had a positive effect on the condition of the wrecks, especially those with wooden structures [11].

Most of the wrecks in Polish sea areas come from World War II [12]. There are sunken passenger ferries, the U-boats, a German aircraft carrier and three wrecks (Steuben, Goya and Wilhelm Gustloff) from the greatest maritime tragedies of all time, where more people died than by the sinking of the Titanic [13]. As an ecological and human safety risk, some wrecks are of particular interest due to the presence of conventional ammunition or fuel-filled tanks [14]. In most cases, the wrecks of large vessels are not affected by human activity, which makes Polish seawaters an attractive place for underwater wreck tourism.

So far, a large number of hobbyist divers and archaeologists have been mainly concerned with the wrecks of ships, but only a few with those of airplanes. Due to the fact that air crashes are accompanied by heavy damage, they result in fragmentation of the wreckage on the seabed. To fill the knowledge gap around aircraft wrecks, the discovery of the German Ju-88 bomber from World War II is of particular scientific interest. The Junkers Ju-88 was one of the most famous German aircraft of World War II. It was a fast bomber, subjected to many modifications, and widely used since March 1939. It was used as a reconnaissance aircraft, dive bomber, day and night bomber and, depending on the weapons installed, as a torpedo bomber and fighter. The fuselage was divided into three sections, the wings had rounded tips and were made of duralumin, with engine nacelles at the bottom that moved three-blade propellers.

The Polish sea area of over 30,000 km² is not fully covered by bathymetric measurements, and objects are still being discovered. Even using a modern sonar system, a full coverage mapping of such a large area with sufficient quality is still very time-consuming. Remote sensing techniques, especially acoustic, as non-invasive and non-destructive measurement methods, have played an extremely important role in the study of the marine environment for several decades, providing an impressive coverage of spatial data used for its observation and monitoring [15–17]. Thanks to them, archaeologists can obtain unique data, unattainable with the use of traditional archaeological excavation techniques [18]. Techniques for measuring the depth and visualizing the bottom surface have developed dynamically since the invention of the first acoustic sounder in the 1920s [19]. Over the last decades, thanks to a steady increase in the number of multibeam echo sounders, more accurate maps of the seafloor surface featuring wrecks have been obtained [4]. Today, these devices are the most effective method of seafloor mapping [20]. This technology allows the generation of information about the wrecks located at great depths.

The paper presents an example of the examination of an underwater object detected in the Polish part of the Baltic Sea. This has been already proven by many authors. Hydroacoustic measurements allow us to detect and survey shipwrecks remotely, to analyze and identify the target without diving operations. The main aim of the article is to present the results of remote sensing surveys that were carried out at the site of a newly discovered underwater object. The author's approach to the survey of the wreck with particular instruments configuration and sequence of their usage has been demonstrated. Successful identification of the airplane wreck confirmed the usefulness and effectiveness of the use of the appropriate set of sensors and adopted methodology.

2. Materials and Methods

2.1. Study Area

In February 2013, hydroacoustic surveys were conducted by the vessel Arctowski from the Hydrographic Support Squadron of the Polish Navy in the framework of the HELCOM Baltic Sea Environment Protection Commission. The aim of the cruise was to survey the area north of the town of Łeba using a multibeam echo sounder and to detect and verify underwater objects along the Polish coast. During the acoustic mapping, on the eastern coast of Poland, an airplane wreck was detected at a depth of 20–30 m, a few nautical miles north of the Stilo lighthouse (Figure 1).

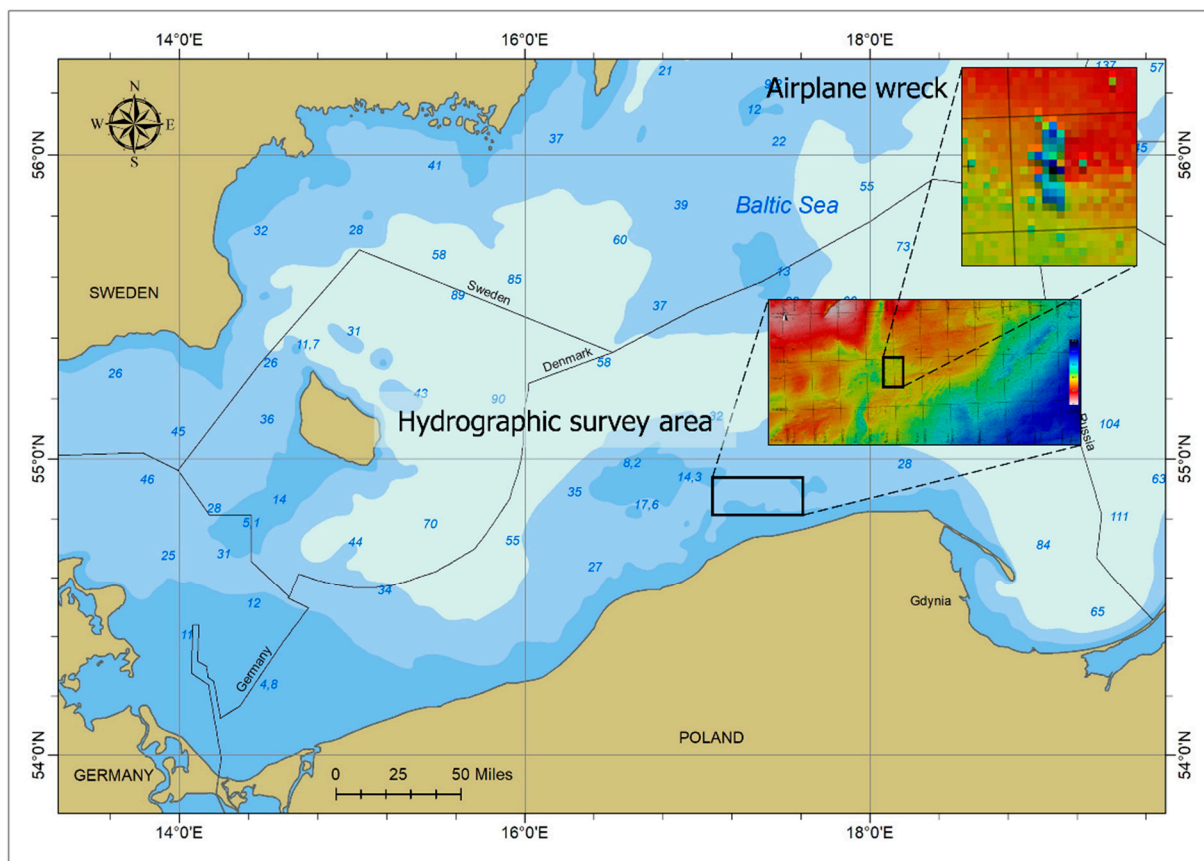


Figure 1. Location of study area where the survey was conducted by *Arctowski*.

The first survey data showing the new wreck lying on the seafloor were recorded by means of multibeam echo sounder system (Figure 2). This device performs a multi-point depth measurement in a wide strip of the bottom, and the obtained data make it possible to “build” a three-dimensional, high-resolution point cloud of the surface bottom and visualize objects detected during the survey [21]. A great advantage of the multibeam echo sounder is the possibility of full data coverage of the designated study area, that is, the complete acoustic ensonification of the seabed [22,23]. Figure 2 shows the swath width during the ship’s passage on the survey line no. 70, where a new object—the wreckage—was discovered. Unfortunately, on the basis of such a data it was impossible to determine what type of underwater object we were dealing with.

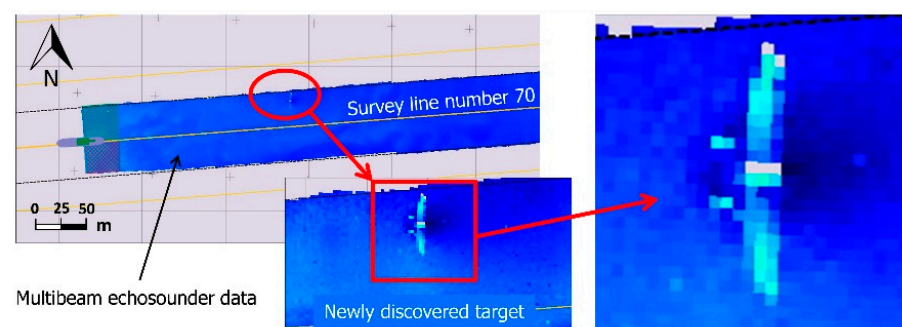


Figure 2. The moment of detecting the wreck by means of MBES on the survey line number 70.

2.2. Survey Design and Instrumentation

After the discovery of the airplane wreck, a detailed survey was conducted in order to determine the degree of risk to safe navigation in this water area. The main purpose of the

research was to determine the position of the object, estimate its geometrical dimensions, measure the depth above the object, determine the bottom type and characterize the orientation of the wreck on the seafloor [24]. The main devices used in the research were a multibeam echo sounder EM-3002D, side-scan sonar Klein 3900, scanning sonar version 1071 (Kongsberg Simrad Mesotech) and a remotely operated vehicle Falcon SAAB SeaEye (Figure 3).



Figure 3. Instruments used for surveying the airplane wreck: (a) multibeam echo sounder EM-3002D; (b) side-scan sonar Klein 3900 System; (c) scanning sonar ver. 1071; (d) remotely operated vehicle Falcon SAAB SeaEye.

2.2.1. Bathymetric Survey Planning and Data Acquisition

In order to perform a detailed hydrographic survey, on the basis of the initially obtained data, a study site was designated. The area was covered with a grid of survey lines with the directions of 70–250°. The angular swath coverage established for this survey was $Sw = \pm 50^\circ$ (in total 100°), which resulted in a horizontal range of about 70 m. The spacing between the survey lines was set to 56 m, thus providing a 20% overlap between adjacent swathes (Figure 4). The second grid of survey lines was oriented in the 160–340° direction. In this way, 200% bottom coverage was ensured. At this stage, the main goal of the research was to obtain a full coverage map of the research area.

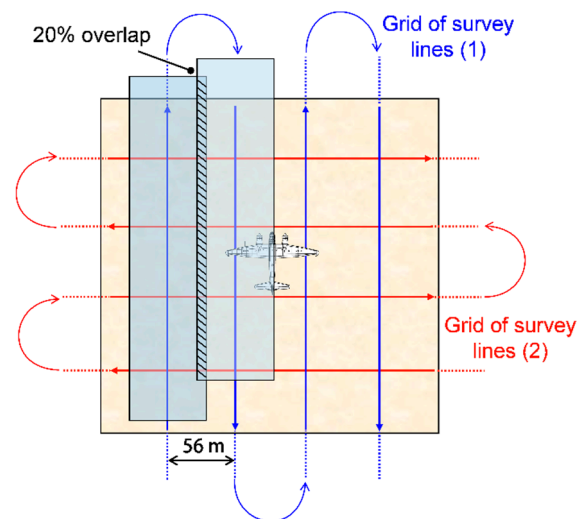


Figure 4. Grids of bathymetric survey lines planned in the wreck site.

In the first stage, the bathymetric measurements were performed using the Kongsberg Maritime EM-3002D multibeam echo sounder system with two sonar heads installed at the ship's hull. The mounting tilt angle of a single head was 40° . We used 254 receive beams spaced in an equidistant pattern within the specified coverage. The spacing between soundings as well as the acoustic footprints can be set nearly constant over the swath in order to provide a uniform and high detection and mapping performance [25,26]. Survey

project settings applied to the bathymetric survey are presented in Table 1, and basic MBES specifications are shown in Table 2.

Table 1. Survey project settings applied to bathymetric measurements of the wreck site.

Parameter	Value
Total swath coverage	100°
Horizontal range	70 m
Line spacing	56 m
Overlap	20%
Bottom coverage	200%
Survey speed	5 knots

Table 2. Technical specification of the multibeam echo sounder EM 3002D.

Specifications	
Frequency	300 kHz
Max ping rate	40 Hz
Beamwidth	1.5° × 1.5°
Depth resolution	1 cm
Pulse length	150 µs
Tilt angle	40°

To allow a proper beam forming, sound velocity was received by the mini Valeport sound velocity sensor (SVS) mounted on the blister in close proximity to the sonar heads. Data on the Surface Sound Speed was recorded and sent to the system in real time. The multi-purpose system Seapath 300 was used in the study, ensuring the exact position, course over ground and motion compensation. The system has two built-in GNSS receivers to measure the position and speed of the ship and the Motion Reference Unit MRU5 for measuring pitch, roll and heave. Before starting the bathymetric measurements, the velocity of sound in the water column was measured. For this purpose, the Midas SVX Valeport probe equipped with conductivity, temperature and depth sensors was used. For planning, recording and processing of bathymetric data, the Qinsy software package by QPS (Quality Integrated Navigation System) and Qloud version 2.3 was applied. The speed of the hydrographic ship during the survey was 5 knots and the research was carried out in good weather conditions with wind speed below 2 knots and 0.2 m wave height.

Multibeam echo sounder systems are characterized by the ability to fully insonify the bottom surface, provide high-resolution bathymetric data and the ability to accurately reproduce the actual shape of the bottom [27]. In order to build a high-resolution image of the wreck and obtain a high detail of three-dimensional imaging, it is extremely important to know the resolution capabilities of the system that is planned to be used for surveying. Therefore, the sizes of acoustic footprints of individual beams were estimated for given environmental conditions. The width or dimension of the footprint ellipse in the fore-aft direction, for a flat seafloor, is approximately given by a_x :

$$a_x = \frac{2 \cdot z}{\cos \beta} \cdot \tan \frac{\varphi_T}{2}, \quad (1)$$

where a_x is the width of the footprint ellipse in the fore-aft direction, z is the mean depth, β is the beam pointing angle, φ_T is the width of the transmitted beam.

Taking a flat and leveled seafloor, the length of this ellipse in the athwartships direction is approximately given by a_y :

$$a_y = \frac{2 \cdot z}{\cos^2 \beta} \cdot \tan \frac{\varphi_R}{2}, \quad (2)$$

where a_y is the width of the footprint ellipse in the athwartship direction, φ_R is the width of the reception beam in the athwartship direction.

In order to obtain the best measurement resolution and appropriate detail of the image, a reduced swath angle of MBES was used, i.e., $\pm 50^\circ$. Such an opening angle of the multibeam transducer ensured proper survey efficiency and, at the same time, the required resolution of the measurement. The survey lines were planned in such a way that when passing directly over the wreckage, MBES recorded the data using vertical beams with the smallest beamwidth. The initial examination of the wreck with MBES enabled the determination of points of minimum depths in the wreck site, planning of tracks for side-scan sonar survey, and visualization of the wreckage remains and seafloor features.

2.2.2. Sonar Survey Planning and Data Acquisition

For further exploration, a side-scan sonar was used, which offers higher imaging resolution of the seafloor surface. The side-scan sonar (Figure 3b) measures the time from the moment of transmitting the impulse to the moment of receiving the signal reflected from the bottom and records the amplitude of the received echo [28–31]. SSS allows the identification and verification of detected objects, and thus completes the information collected by the multibeam echo sounder.

The aim of sonar imaging was to record high-resolution data of the seafloor and object. The wreck was examined with the use of SSS operating simultaneously on two frequencies (455 kHz/900 kHz). A Klein 3900 digital sonar (“fish”) was towed on a 200 m kevlar cable and the data were recorded in a computer acquisition system using the SonarPro software. The side-scan sonar 3900 is a high-resolution digital sonar for use in search and recovery missions. The basic technical specifications of the Klein 3900 System are presented in Table 3.

Table 3. Technical specifications of the side-scan sonar Klein 3900.

Specifications	
Frequencies	455 kHz, 900 kHz
Beams	horizontal 0.21° ; vertical 40°
Max range	150 m @ 445 kHz; 50 m @ 900 kHz
Depth rating	200 m
Sensors	Roll, pitch, heading
Options	Pressure sensor

The basic scheme of the sonar examination of the detected wreck was the set of parallel sonar tracks. Several sonar passes were made next to the wreck. The first track was run from one side of the wreck and the second line was followed from the opposite side. Additionally, a survey line at an angle of 45 degrees to the airplane wings was planned. The approximate altitude at which the side-scan was towed over the seafloor (4.3–5.5 m) as well as the right distance from the wreck (15–20 m) resulted in clear and detailed sonar images.

In order to optimize the usefulness of the side scan sonar images, the data were processed with SonarPro software. Raw side-scan sonar data is distorted due to the speed variations in the survey vessel, sonar instabilities and towfish altitude (slat-range distortion). The gain-versus-time (TVG) was set to obtain a uniform level of backscatter throughout the range of interest. Then, the slant range correction was applied to sonar data since uncorrected images are not real representations of the seafloor. After slant range correction, side-scan sonar images were corrected in the along-track direction for variations in ship speed. This correction aimed at delivering images with a 1:1 aspect ratio. Speed variations were corrected by applying calculated ship speed from GPS data.

2.2.3. Scanning Sonar

To ensure the accuracy of the sampling operation, an electronic chart system was used. The aim of this part of the research was to perform a survey with scanning sonar

and to inspect the wreck using ROV. After the ship had been anchored, the scanning sonar was prepared to be placed on the seafloor 10 m from the wreckage. The mobile sonar system includes a sonar head of Kongsberg Simrad Mesotech version 1071, a 150 m cable, an interface box, and a computer with MS-1000 software for data recording and processing. The main advantage of the scanning sonar was its high resolution, related mainly to the high-frequency acoustic signal of the 675 kHz, the beamwidth of $0.9^\circ \times 30^\circ$ and the minimum pulse length of 25 μ s. The sonar specifications used during the survey are shown in Table 4.

Table 4. Technical specifications of the sonar head used during the survey.

Specifications	
Operating frequency	675 kHz
Beam width	$0.9^\circ \times 30^\circ$ Fan
Range	20–25 m
Scan angle	360°
Step size	0.225°
Pulse lengths	25 μ s

The scan angle is 360° and the minimum transducer angular step size is 0.225° . The system has the ability to scan the bottom surface faster at step size 0.5° or 1.0° and higher, although increasing the rotational speed of the transducer causes a decrease in the resolution of the sonar imagery. Sonar data was recorded with the smb extension using the MS 1000, version 5.25 software.

2.2.4. ROV Mission

Visual inspection of the wreckage with the use of an ROV was performed for detailed ground truthing to verify the acoustic images. Video footage was recorded using a TV camera mounted on a remotely operated underwater vehicle. For visual examination of the wreck, a Falcon SAAB SeaEye vehicle was used, consisting of a submersible vehicle, power supply interface, control and steering devices, and a 300 m long cable line with a drum. During the survey, the ROV pilot performed three vehicle dives.

The use of ROVs is widely practiced and, as experience has shown, much more effective than the use of lowered underwater cameras. Photos and videos obtained with this technique provide information on the physical condition of the discovered object, the degree of destruction of the wreck or how deep the wreck is buried with sediments. Based on the video documentation, it will be possible to determine whether there are any fishing nets, or explosives on the wreck or in its vicinity [7].

3. Results

3.1. MBES Data

To process the recorded MBES data, a standard QINSY (QPS) workflow was applied, including data verification, outlier correction by spline filtering, tide correction and sound speed correction. After removing outliers, a regular grid of data was generated with a size of $0.5 \text{ m} \times 0.5 \text{ m}$ (Figure 5).

The bathymetry displayed in Figure 5 is the result of a study around the position of the plane wreck. The depths in the research water area ranged from 24 m to 27 m, and sand was present in the majority of the seafloor [32]. The point cloud images of the wreck presented in Figure 6a,b did not indicate the detection of the airplane wreckage. Only the recording of an additional set of bathymetric data (grid of survey lines 2) and an increase in the density of measurements made it possible to create three-dimensional models of the detected wreck (Figure 6c,d) showing a certain symmetry in the construction.

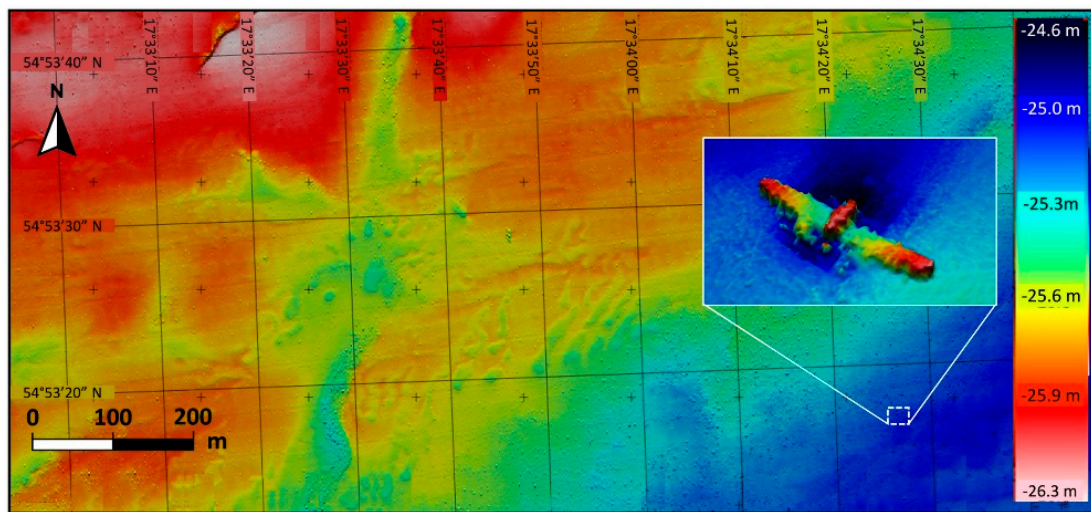


Figure 5. Grid of bathymetric data and location of the wreck prepared based on multibeam echo sounder measurements.

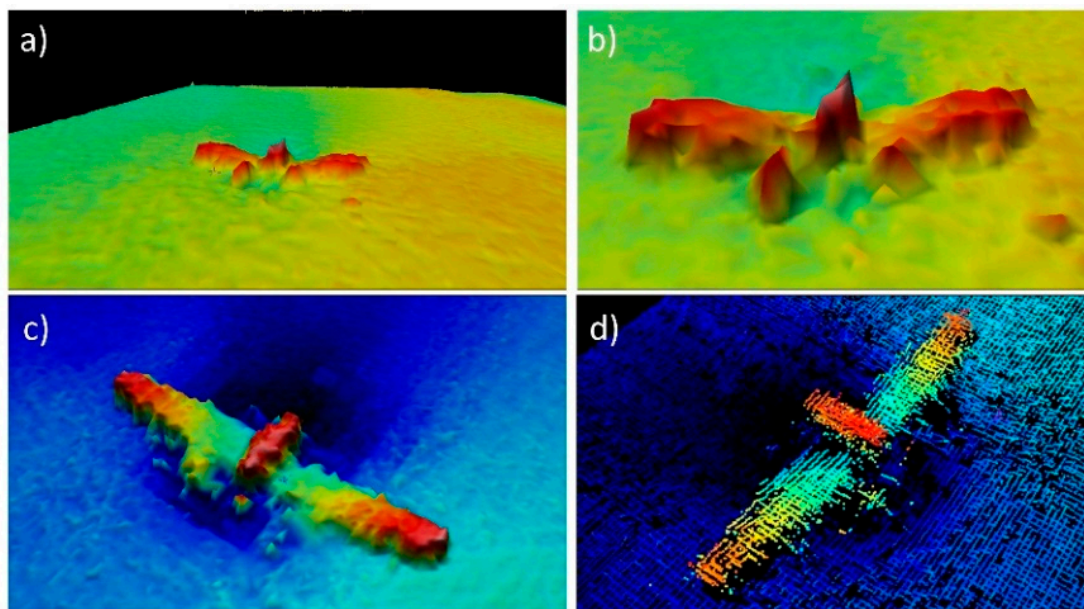


Figure 6. Digital models of the plane wreck: (a,b) models developed based on data recorded during one pass over the wreck; (c,d) models developed based on the increased density of bathymetric data.

The digital bathymetric models of the plane wreckage presented in Figure 6a,b are not very detailed or clear and do not reveal many valuable characteristics that could be used in the object identification process.

3.2. Sonar Data and Results of ROV Inspection

Towing the side-scan sonar at a very low altitude ($F_a = 2$ m) and in close proximity to the wreck resulted in recording a sonogram of negligible value in the process of the wreck's identification (Figure 7a). On the next track line, located 20 m from the wreck, a sonogram was recorded with a set range of $R = 40$ m. The sonar was towed at a speed of $V = 4.3$ knots, however, its altitude was far too high ($F_a = 14$ m). The sonogram obtained in this way (Figure 7b) was also not suitable for identifying the wreck. Figure 7c shows the sonar image recorded at the speed $V = 3.5$ knots and sonar altitude of $F_a = 6.7$ m. In this case, the range was reduced to $R = 30$ m, however the sonar was towed too far from the wreck. Consequently, part of the acoustic shadow did not fit in the display window. With such

imagery, it is not possible to accurately calculate the height of the airplane wing above the bottom. The acoustic images shown in Figure 7 based on the survey lines parallel to the axis of the aircraft wings did not provide sufficient quality for a further identification procedure.

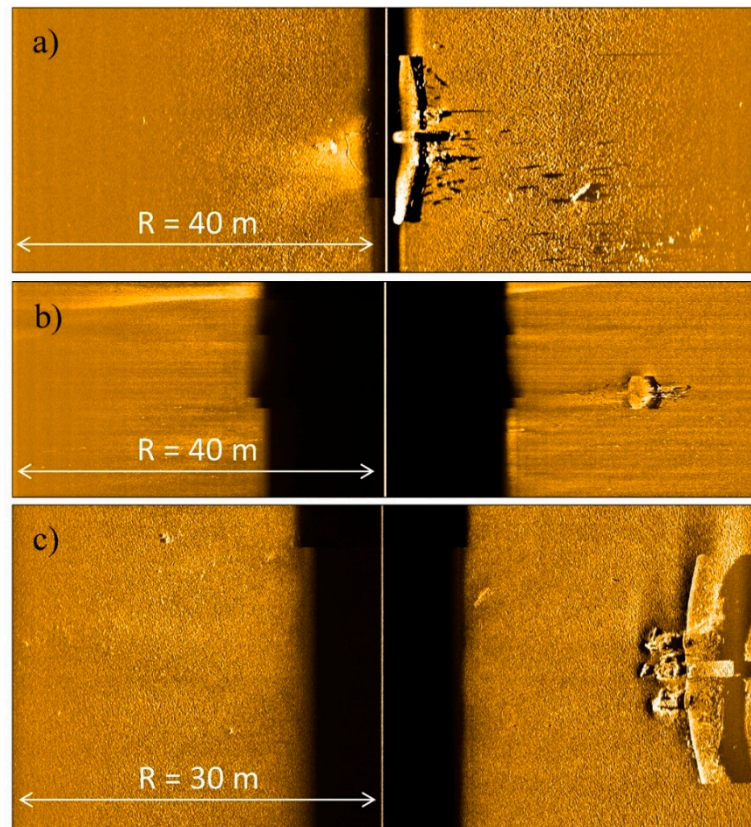


Figure 7. Side scan sonar data of little utility and value: (a) sonar is flying too low and too close to the wreckage; (b) sonar is flying too high above the bottom; (c) sonar is flying too far from the wreckage.

It was decided to plan track lines oriented perpendicular to the axis of the plane's wings. The first line was designed to be located approximately 20 m from the aircraft cockpit. The range was set to $R = 40$ m to visualize the wreck in the middle of starboard channel display. The sonar altitude was $F_a = 5.5$ m above the seafloor surface, with a towing speed of $V = 3.5$ knots. This time, a recorded sonogram (Figure 8a) clearly indicated what kind of wreck we were dealing with. In order to acquire the image with a greater level of detail, the sonar range was reduced to $R = 30$ m. The altitude of the sonar was also reduced to $F_a = 4.3$ m while maintaining the same towing speed. As a result, a clear and detailed sonogram was recorded (Figure 8b), suitable for use in the wreck's identification process.

According to [27], when examining underwater objects with the use of side-scan sonar, the target (feature, wreck) should be ensonified by an acoustic beam at various angles. For this purpose, we designed the survey lines running parallel to the airplane wings and at an angle of 45 degrees to the wing axis. Sonar images of the wreck were recorded at the towing speed of $V = 3.5$ knots. The results are presented in Figure 9a,b. These are examples of "good quality" data resulting mainly from selected survey parameters (Table 3) and good weather conditions.

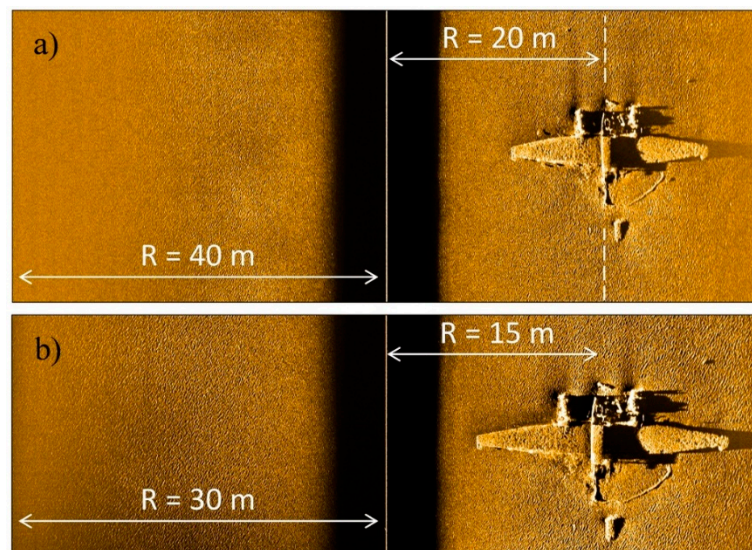


Figure 8. Side scan sonar data of considerable utility and value: (a) sonar is flying 20 m from the wreckage, range $R = 40\text{ m}$; (b) sonar is flying 15 m from the wreckage, range $R = 30\text{ m}$.

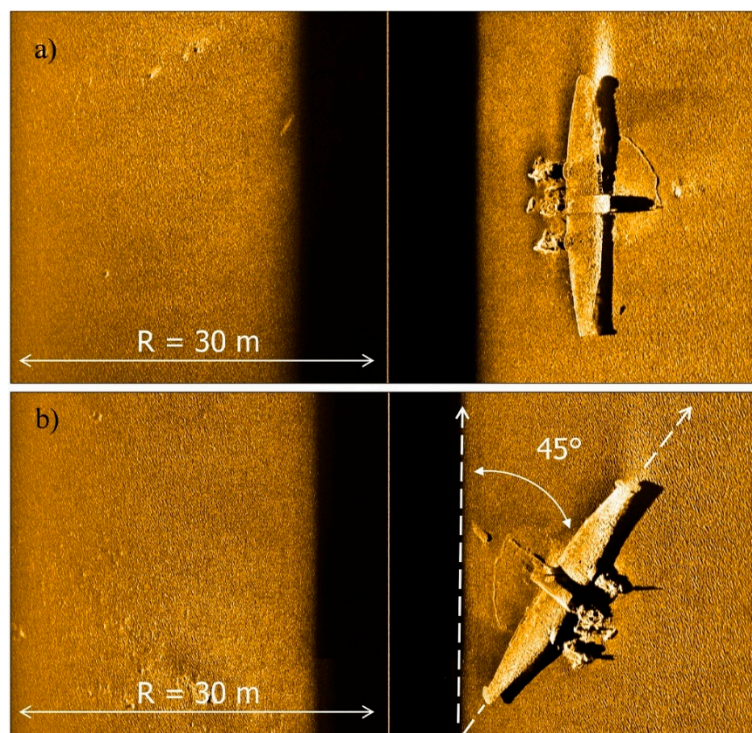


Figure 9. Side scan sonar data recorded with the Klein 3900 system: (a) sonar track line parallel to the axis of the airplane wings; (b) sonar track line at the angle of 45 degrees to the axis of the airplane wings.

After finishing the bathymetric and sonar survey, we commenced with mapping the object using scanning sonar and ROV. First, the scanning sonar MS 1000 Kongsberg Maritime was placed on the bottom in close proximity to the wreck. Data were recorded with a minimum transducer angular step of 0.225° for the highest resolution. In the last stage of the study, in order to get a visual overview, the ROV was deployed. No material was removed and ROV recorded almost an hour of footage of considerable value (Figure 10). The obtained movie documentation was an invaluable aid in the identification of the wreck. An inspection carried out with the use of an ROV allowed us to determine the current

condition of the wreck, the degree of cover with bottom sediments, the presence and quantity of nets, and the presence of ammunition and explosives.

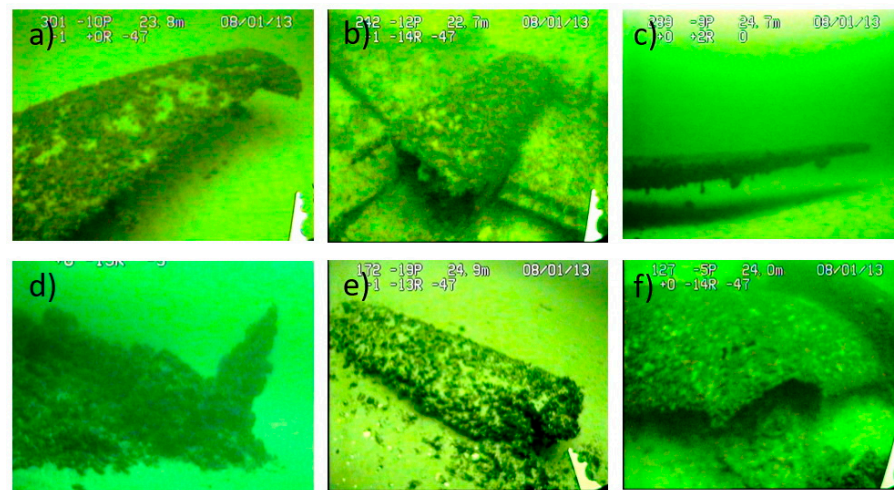


Figure 10. Video data recorded with the ROV camera: (a) part of the right wing; (b) part of the cockpit; (c) part of the left wing; (d) engine propeller; (e) part of the tail detached; (f) engine cover on the right wing.

4. Discussion

Identifying a shipwreck or airplane wreck is a complex task, and, in many cases, it is more difficult than discovering it [33]. Berg [34] and Keatts [35] claim that the wreck might be successfully identified based on the artifacts found in it. A hull number or the name of the vessel clearly confirms the identity of the underwater findings. Harpster [36] believes that the letters or numbers on the vessel's bell may suggest the name and affiliation of the shipwreck. This requires the use of divers. Grabiec and Olejnik [37] claim that the most effective method of wreck recognition is the use of unmanned vehicles. The authors believe that only photographic or TV images of the wreck provide 100% certainty in the identification process.

Wreck identification is a multi-stage process of establishing the identity based on the collected photos and drawing documentation, analysis of historical facts, results of bathymetric and sonar measurements, diving inspection and movie material recorded with a TV camera mounted, for example, on an ROV vehicle [38]. In the process of identifying the wreck, the method of comparative analysis was applied. Sonar images of the airplane wreck were compared with the source documentation. The higher the compliance of the compared geometric features, the greater the probability of a positive identification of the airplane wreck. The consistency of dimensions, similar shapes of the object, analogies in the location, and the shape and size of the characteristic hull parts were analyzed. Initially, four types of aircraft were chosen, the sizes of which, in particular the wingspan, corresponded to the dimensions of the discovery (Figure 11).

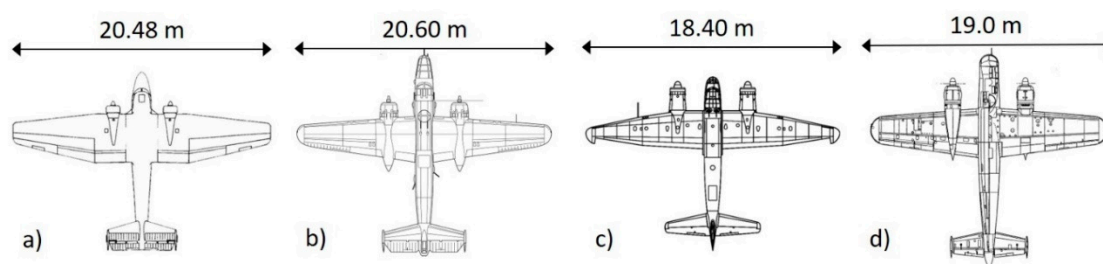


Figure 11. Four types of aircraft selected in the first phase of identification: (a) Szcz-2 aircraft; (b) B-25 Mitchell aircraft; (c) Junkers Ju-88 aircraft; (d) Dornier Do 217 aircraft.

The Szcze-2 was a Soviet transport aircraft from World War II, developed in 1942 as a light transport aircraft, especially for transporting paratroopers. The B-25 Mitchell was a World War II American medium bomber used as a horizontal bomber. In turn, the Junkers Ju 88 was a German, twin-engine, fast bomber from World War II, one of the most versatile aircraft of this conflict [39]. The last one, the Dornier Do 217, was a medium bomber and night fighter of German construction, also from World War II [40,41]. Rough measurements of the wreckage using sonar data showed that we were dealing with an aircraft with a wingspan of about 20 m. Analysis of the plating and shape of the wings presented some inconsistencies, which resulted in the rejection of the B-25 Mitchell bomber (Figure 12).

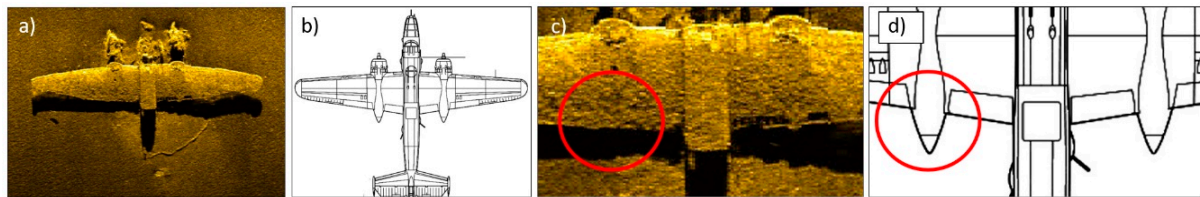


Figure 12. Comparison of the sonar image of the wreck with the B-25 Mitchell bomber: (a) sonar imagery of the wreck; (b) the floor plan of the B-25 Mitchell bomber; (c) identifying the wing feature in the sonar image; (d) identification of the engine on the construction plans.

Then, the sonar image of the wreck was compared with the silhouette of the Soviet Szcze-2 transport aircraft. The wingspan was similar, but their shape differed. There was a large difference in distance between the wing engines. The distance between engines in the sonar image was 5.5 m, while in fact on the construction plans this distance was approximately 4.7 m (Figure 13). This difference influenced the decision that the Szcze-2 aircraft should not be taken into account.

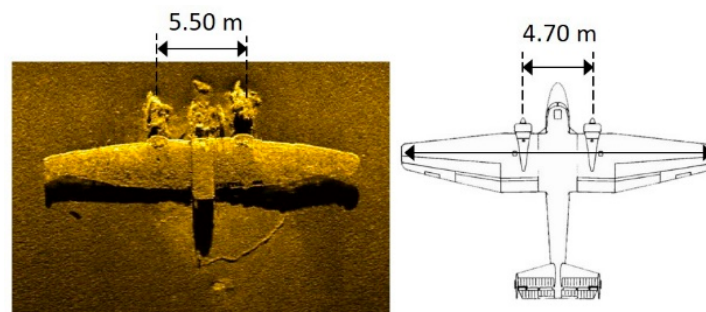


Figure 13. Comparison of the distance between the wing-mounted engines based on sonar data and technical data of the Szcze-2 aircraft.

The Dornier Do 217 aircraft with a wingspan of 19 m was selected. A thorough analysis of the wing structure and sonar images were compared with the construction diagrams. The aileron of the wings formed a straight line in this model of the aircraft (Figure 14b). A side-scan sonar image (Figure 14a) showed that there is a breakpoint in the ailerons. The Dornier plane had wings that formed a single plane in the vertical section (Figure 15a). The multibeam echo sounder data shows that the wings of this wreck do not lie in one plane. The wings connect with the fuselage at a slight angle (Figure 15b). Thus, the hypothesis that it was a Dornier was rejected.

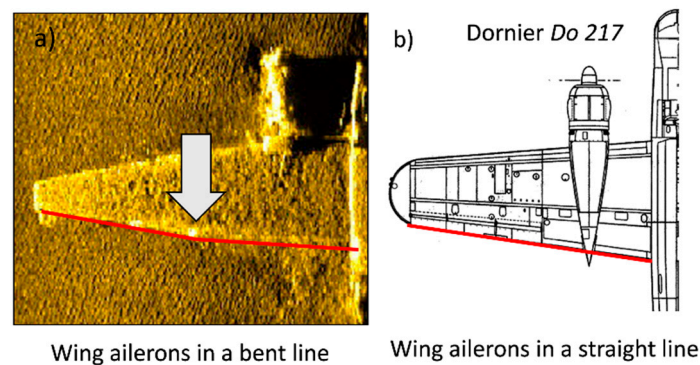


Figure 14. Comparison of the shape and arrangement of the wing ailerons: (a) side-scan sonar image of the airplane wreck's wing, (b) plane projection of the Dornier Do 217.

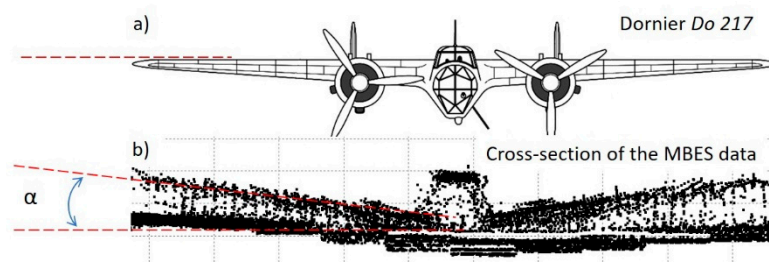


Figure 15. Comparison of the wing arrangement and wingspan: (a) wing arrangement of the Do 217; (b) wing arrangement of the discovered wreck of plane, vertical cross-section of the multibeam echo sounder data.

The Junkers Ju-88 bomber was characterized by a wingspan of 18 m 25 cm. This dimension did not match our measurements. However, the first models had a wingspan of 18 m, and subsequent models were produced with wings extended to 20 m 8 cm [42–45]. Based on the results of the bathymetric measurements (Figure 16a) and side-scan sonar measurements (Figure 16b) the wingspan was about 20 m. Additionally, the distance between the engines on the bomber's wings was measured and compared. The results of the comparisons were consistent, and they differed only by 5 cm (Figure 16c).

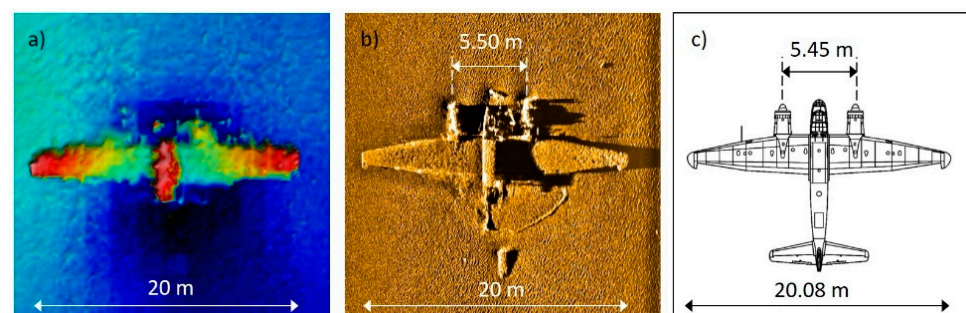


Figure 16. Comparison of the wingspan and distance between engines: (a) data recorded with MBES; (b) sonar imagery and dimensioning; (c) actual dimensions of the Junkers Ju 88.

Comparative analysis of the wingspan, the arrangement of engines and the shape of the cockpit showed compliance with these features. Then the cross-section of the bathymetric point cloud of the wreckage was compared with the front view of the bomber. The data from the multibeam echo sounder clearly shows an airplane wreck, the wings of which were slightly raised (Figure 17). The Junkers Ju-88, unlike the Dornier Do 217, was characterized by such a position of the wings.

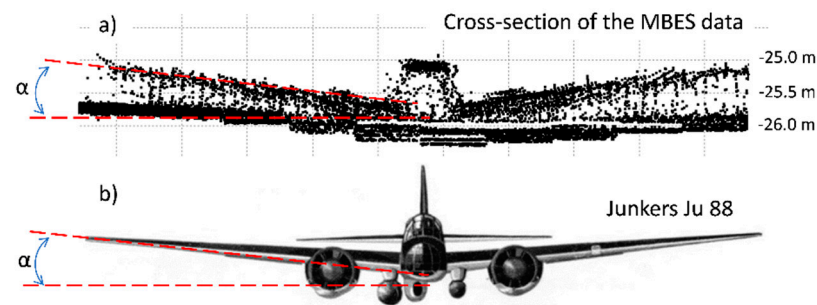


Figure 17. Comparison of the wing elevation angle of the wreck: (a) wing arrangement of the airplane wreck, a vertical cross-section of the MBES data; (b) actual model of the Junkers Ju-88.

The first dozen Ju 88A-4s were equipped with wooden propellers made of refined laminated wood [46]. Part of the preserved propeller of the wreckage is shown in Figure 18. The ROV recorded video documentation of the wreckage and its surroundings. The video material made it possible to identify several characteristic elements of the wreck. The photos showed the bomber's entire wings without ailerons, with the pilot's seat and engine nacelles (Figure 18).

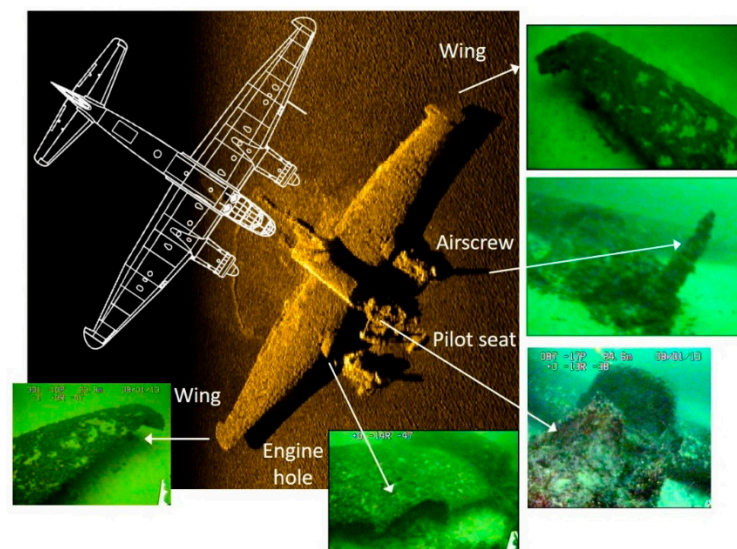


Figure 18. Identification of selected parts of the wreck of bomber on the basis of data recorded with ROV and side-scan sonar.

The results of side-scan sonar imaging, bathymetric survey and ROV inspection made it possible to establish certain facts. Based on the bathymetric measurements conducted with MBES, the height of the wreck is 120–140 cm above the seafloor surface, the wings' orientation at the bottom is 0–180° and the wingspan is 20 m. Side-scan sonar data and ROV footage show that the wreck is free from fishing nets, and fragments of propellers have been preserved. There are two engines without covers, a damaged cockpit and a visible pilot's seat.

Based on an analysis of the survey results, the discovered object is the wreckage of an airplane. The wingspan and the shape of the wings, the number and layout of the engines, as well as the cockpit size and other features indicated that it is a German Ju-88 bomber in the A-4 version. Data from a multibeam echo sounder allowed for the detection of the object on the seafloor, but only the use of side-scan sonar confirmed the wreckage of the historic World War II Junkers airplane.

The results of the wreck's examination indicate that the MBES, SSS and ROV are effective sensors not only for routine hydrographic works but also for an archaeological site

survey. Data obtained with these instruments constitute key documentation in the wreck's identification. The wreck does not pose a danger for navigation, and at the same time, it can be a unique attraction for divers, historians and enthusiasts of underwater exploration.

5. Conclusions

The aim of this paper was to show how acoustic remote sensing is used to search, survey and identify an airplane wreck. The proposed approach involves the application of multibeam echo sounder and side-scan sonar technology, an appropriate methodology that enabled the collection of high-resolution remote sensing data that contributed to the identification of the wreck. The identification level allows us to state that the examined object is the wreck of a Ju-88 bomber. The compliance of the research material with the archival documentation, building plans, and historical photos fully justifies the above statement.

This article demonstrated that successful identification of an airplane wreck is possible without involving a team of divers. This is especially important in terms of human safety or survey operation costs. Side-scan sonar enabled obtaining remarkably clear and contrasting sonar imagery with a high level of detail. The paper traced the importance of remote sensing techniques and, in particular, MBES, SSS as well as ROV as efficient and optimized mapping tools. This was exemplified through the project survey and the different techniques employed. The results generated from the remote sensing hydrographic works are hugely important due to their contribution to World War II history, but also to the safety of navigation in the Polish coastal water areas.

Funding: This research received no external funding.

Acknowledgments: The author would like to thank the crew of the Polish Navy Hydrographic Ship *Arctowski*, for their dedication, exemplary performance of tasks and fantastic atmosphere onboard during over 18 years of service.

Conflicts of Interest: The author declares no conflict of interest.

References

1. UNESCO Convention on the Protection of the Underwater Cultural Heritage. 2007. Available online: <https://unesdoc.unesco.org/ark:/48223/pf0000152883> (accessed on 13 August 2021).
2. Shipwrecks. Global Foundation for Ocean Exploration. Available online: <https://www.engineeringfordiscovery.org/education/shipwrecks/> (accessed on 26 January 2022).
3. IOC-UNESCO. *Global Ocean Science Report—The Current Status of Ocean Science around the World*; Valdés, L., Crago, M., Enevoldsen, H., Garcia, H.E., Horn, L., Inaba, K., Inniss, L., Isensee, K., Keeley, B., Mees, J., et al., Eds.; UNESCO Publishing: Paris, France, 2017. Available online: <https://en.unesco.org/gosr> (accessed on 21 February 2022).
4. Mayer, L.; Jakobsson, M.; Allen, G.; Dorschel, B.; Falconer, R.; Ferrini, V.; Lamarche, G.; Snaith, H.; Weatherall, P. The Nippon Foundation—GEBCO Seabed 2030 Project: The Quest to See the World's Oceans Completely Mapped by 2030. *Geosciences* **2018**, *8*, 63. [CrossRef]
5. Koutsi, D.; Stratigea, A. Unburying Hidden Land and Maritime Cultural Potential of Small Islands in The Mediterranean for Tracking Heritage-Led Local Development Paths. *Heritage* **2019**, *2*, 62. [CrossRef]
6. Argyropoulos, V.; Stratigea, A. Sustainable Management of Underwater Cultural Heritage: The Route from Discovery to Engagement—Open Issues in The Mediterranean. *Heritage* **2019**, *2*, 98. [CrossRef]
7. Hac, B.; Sarna, O. *General Methodology of Oil Removal Operations on Baltic Shipwrecks*; Report; The MARE Foundation: Warsaw, Poland, 2021; ISBN 978-83-959773-0-5. Available online: http://fundacjamare.pl/file/repository/2021_MARE_METODYKA_oczyszczania_wrakow_RAPORT_pl.pdf (accessed on 20 July 2022).
8. Counteracting the Threats Resulting from the Deposit of Hazardous Materials on the Baltic Sea [in Polish]. Information on the inspection results. Registration number: 192/2019/P/19/068/LGD. Supreme Chamber of Control, Branch office in Gdańsk. Warsaw 2020. Available online: <https://www.nik.gov.pl/kontrola/P/19/068/> (accessed on 14 June 2022).
9. Geraga, M.; Papatheodorou, G.; Ferentinos, G.; Fakiris, E.; Christodoulou, D. The study of an ancient shipwreck using marine remote sensing techniques, in Kefalonia Island (Ionian Sea), Greece. *Archaeol. Mariti. Mediterr.* **2015**, *12*, 183–200.
10. Bates, C.R.; Lawrence, M.; Dean, M.; Robertson, P. Geophysical Methods for Wreck-Site Monitoring: The Rapid Archaeological Site Surveying and Evaluation (RASSE) programme. *Int. J. Naut. Archaeol.* **2011**, *40*, 404–416. [CrossRef]

11. Analysis of the Pollution of the Baltic Sea, with Particular Emphasis on Ships Sunk during World War I and II. Information on Pollution Action Taken by the European Parliament, the Helsinki Commission and Other Governments [in Polish]. Opinions and Expertise OE-364, Analysis, Documentation and Correspondence Office. Chancellery of the Senate, Warsaw 2021. Available online: <https://www.senat.gov.pl/gfx/senat/pl/senatekspertyzy/6049/plik/oe-364.pdf> (accessed on 14 March 2022).
12. *Initial Assessment of the Marine Water Environment of the Polish Baltic Sea Zone [In Polish]—Report to the European Commission of the Marine Branch IMGW-PIB in Gdynia*; Krzymiński, W. (Ed.) IMGW: Gdynia, Poland. Available online: http://www.gios.gov.pl/bip/zalaczniki/konsultacje_spoleczne/folder_C/wstepna_ocena_stanu_srodowiska_wod_morskich_wyniki_konsultacji_i_uzgodnien.pdf (accessed on 11 November 2021).
13. Poleszak, S. (Ed.) *Wrecks of the Baltic Sea. A Guide for Divers*; Wydawnictwo Książki Nurkowe; Oficyna Wydawnicza Eliza Poleszak: Gdynia, Poland, 2005; p. 43. ISBN 83-920563-1-0. (In Polish)
14. Hac, B. Retrieval activities on the Franken shipwreck. *Bull. Marit. Inst. Gdańsk* **2018**, *33*, 172–177. [\[CrossRef\]](#)
15. Godø, O.R.; Tenningen, E. Remote Sensing. In *Computers in Fisheries Research*; Megrey, B.A., Moksness, E., Eds.; Springer: Dordrecht, The Netherlands, 2009. [\[CrossRef\]](#)
16. Strong, J.A.; Elliott, M. The value of remote sensing techniques in supporting effective extrapolation across multiple marine spatial scales. *Mar. Pollut. Bull.* **2017**, *116*, 405–419. [\[CrossRef\]](#) [\[PubMed\]](#)
17. Unninayar, S.; Olsen, L.M. Monitoring, observations, and remote sensing—Global dimensions. In *Encyclopedia of Ecology*; Academic Press: Oxford, UK, 2008; pp. 2425–2446. [\[CrossRef\]](#)
18. Rindfuss, R.R.; Stern, P.C. Linking Remote Sensing and Social Science: The Need and the New Challenges. In *People and Pixels: Linking Remote Sensing and Social Science*; National Academy Press: Washington, DC, USA, 1998; pp. 1–28. [\[CrossRef\]](#)
19. Mayer, L.A. Frontiers in Seafloor Mapping and Visualization. *Mar. Geophys. Res.* **2006**, *27*, 7–17. [\[CrossRef\]](#)
20. Gaida, T.C.; Mohammadloo, T.H.; Snellen, M.; Simons, D.G. Mapping the Seabed and Shallow Subsurface with Multi-Frequency Multibeam Echosounders. *Remote Sens.* **2020**, *12*, 52. [\[CrossRef\]](#)
21. IHO—International Hydrographic Organization. *S-44: IHO Standards for Hydrographic Surveys. Special Publication No. 44—6.0.0. ed.*; International Hydrographic Bureau: Monte Carlo, Monaco, 2020; 41p. Available online: https://iho.int/uploads/user/pubs/standards/s-44/S-44_Edition_6.0.0_EN.pdf (accessed on 19 June 2022).
22. Martí, A.; Portell, J.; Amblas, D.; de Cabrera, F.; Vilà, M.; Riba, J.; Mitchell, G. Compression of Multibeam Echosounders Bathymetry and Water Column Data. *Remote Sens.* **2022**, *14*, 2063. [\[CrossRef\]](#)
23. Mohammadloo, T.H.; Geen, M.; Sewada, J.S.; Snellen, M.; Simons, D.G. Assessing the Performance of the Phase Difference Bathymetric Sonar Depth Uncertainty Prediction Model. *Remote Sens.* **2022**, *14*, 2011. [\[CrossRef\]](#)
24. Grządziel, A. Baltic Titanics—History and current state. *Marit. Rev.* **2005**, *6*, 13–26. (In Polish)
25. Grządziel, A.; Wąż, M. Estimation of Effective Swath Width for Dual-Head Multibeam Echosounder. *Annu. Navig.* **2016**, *23*, 173–183. [\[CrossRef\]](#)
26. Grządziel, A.; Wąż, M. Multibeam Echosounder System in Bathymetric Survey of Planned Shipping Routes [in Polish]. *Logistyka* **2014**, *6*, 4250–4256.
27. IHO C-13. *Manual on Hydrography*, 1st ed.; International Hydrographic Organization: Monte Carlo, Monaco, 2011.
28. Fish, J.P.; Carr, H.A. *Sound Underwater Images. A Guide to the Generation and Interpretation of Side-Scan Sonar Data*; Lower Cape Publishing: Orleans, France, 1990; 188p.
29. Wu, Z.; Yang, F.; Tang, Y. Side-scan Sonar and Sub-bottom Profiler Surveying. In *High-resolution Seafloor Survey and Applications*; Springer: Singapore, 2021. [\[CrossRef\]](#)
30. Wang, Q.; Wu, M.; Yu, F.; Feng, C.; Li, K.; Zhu, Y.; Rigall, E.; He, B. RT-Seg: A Real-Time Semantic Segmentation Network for Side-Scan Sonar Images. *Sensors* **2019**, *19*, 1985. [\[CrossRef\]](#) [\[PubMed\]](#)
31. Georgiou, N.; Dimas, X.; Fakiris, E.; Christodoulou, D.; Geraga, M.; Koutsoumpa, D.; Baika, K.; Kalamara, P.; Ferentinos, G.; Papatheodorou, G. A Multidisciplinary Approach for the Mapping, Automatic Detection and Morphometric Analysis of Ancient Submerged Coastal Installations: The Case Study of the Ancient Aegina Harbour Complex. *Remote Sens.* **2021**, *13*, 4462. [\[CrossRef\]](#)
32. Jaśniewicz, D.; Klusek, Z.; Brodecka-Goluch, A.; Bolałek, J. Acoustic investigations of shallow gas in the southern Baltic Sea (Polish Exclusive Economic Zone): A review. *Geo-Mar. Lett.* **2019**, *39*, 1–17. [\[CrossRef\]](#)
33. Huang, J. Maritime archaeology and identification of historic shipwrecks: A legal perspective. *Marine Policy* **2014**, *44*, 256–264. [\[CrossRef\]](#)
34. Berg, D. *Shipwreck Diving, Instant Downloadable E-Book*; Aqua Explorers: Baldwin, NY, USA, 2015; p. 90. ISBN1 # 10096161675X. ISBN2 -10 096161675X.
35. Keatts, H.; Skerry, B. *Complete Wreck Diving: A Guide to Diving Wrecks*, 1st ed.; Aqua Quest Publications: Locust Valley, NY, USA, 1999; p. 270. ISBN -10 0922769389.
36. Harpster, M. Shipwreck Identity, Methodology, and Nautical Archaeology. *J. Archaeol. Method Theory* **2013**, *20*, 588–622. [\[CrossRef\]](#)
37. Grabiec, D.; Olejnik, A. Searching for and identifying underwater objects. In *Baltic Wrecks: Guide for Divers*; Poleszak, S., Ed.; Eliza Poleszak: Gdynia, Poland, 2005; pp. 81–105. ISBN 83-920563-1-0.
38. Grządziel, A. Using side scan sonar imagery to identify the wrecks. In *The II Hydrographic Workshop, Pomeranian Science and Technology Park*; Hydrographic Support Squadron of the Polish Navy: Gdynia, Poland, 2008.
39. Sobczak, K. *Encyclopedia of World War II*; Wydawnictwo Ministerstwa Obrony Narodowej: Warszawa, Poland, 1975; p. 793. (In Polish)

-
40. Marud, W.; Zieliński, T. *Aviation in Air War. Concepts. History. Present*; Wydawnictwo Naukowe PWN: Warszawa, Poland, 2022; p. 350. ISBN 9788301204792. (In Polish)
 41. Królikiewicz, T. *Polish Plane and Colour*; Wydawnictwo Ministerstwa Obrony Narodowej: Warszawa, Poland, 1981; p. 198. ISBN 8311065462.
 42. Goss, C. *Junkers ju 88 the Luftwaffes Most Versatile Aircraft*; Frontline Books: London, UK, 2017; p. 160. ISBN 9781848324756. (In Polish)
 43. Murawki, M.J.; Ryś, M. *Junkers Ju 88 vol. I*; Kagero: Lublin, Poland, 2014; p. 120. ISBN 9788364596117. (In Polish)
 44. Weal, J. *Junkers Ju 88 Kampfgeschwader on the Russian Front*; Bloomsbury Publishing PLC: London, UK, 2010; p. 96. ISBN -10 1846034191.
 45. Donald, D. *Bombers of World War II*. Brown Packaging Books Ltd.: London, UK, 1998; p. 44, ISBN 1-56799-683-3.
 46. Ledwoch, J. *Junkers Ju 88*; A.J.-Press: Gdańsk, Poland, 1992; p. 44. ISBN -10 0867-7867.